SOME APPLICATIONS OF NASTRAN TO THE BUCKLING OF THIN CYLINDRICAL SHELLS WITH CUTOUTS

By Jerry G. Williams and James H. Starnes, Jr.
NASA Langley Research Center

SUMMARY

The buckling of isotropic and waffle stiffened circular cylinders with and without cutouts was studied using NASTRAN's Rigid Format 5 for the case of axial compressive loading. The results obtained for the cylinders without cutouts are compared with available reference solutions. The results for the isotropic cylinders containing a single circular cutout with selected radii are compared with available experimental data. For the waffle stiffened cylinder, the effect of two diametrically opposed rectangular cutouts was studied. A DMAP alter sequence was used to permit the necessary application of different prebuckling and buckling boundary conditions. Advantage was taken of available symmetry planes to formulate equivalent NASTRAN model segments which reduced the associated computational cost of performing the analyses. Limitations of the applicability of NASTRAN for the solution of problems with nonlinear characteristics are discussed.

INTRODUCTION

Thin-walled circular cylindrical shells are commonly subjected to compressive type loading, and hence, buckling of these structures must be considered as a possible failure mode. The presence of cutouts in the sides of these structures can significantly reduce their load carrying capability as well as complicate the buckling analysis.

A limited number of experimental (refs. 1, 2, and 3) and finite-difference analytical (refs. 3 and 4) studies of the effects of cutouts on cylindrical shell buckling behavior have been reported. These investigations have been limited to isotropic cylinders with unreinforced circular cutouts and reinforced and unreinforced rectangular cutouts.

Current activities at the Langley Research Center include testing and analysis of small scale isotropic cylinders and very large waffle stiffened cylinders with cutouts. The NASTRAN finite-element program was used to perform the analytical studies of the buckling characteristics of these cylinders. Analytical studies were made of an isotropic cylinder with a single circular cutout at the midlength of the cylinder and a waffle stiffened cylinder with two diametrically opposed rectangular cutouts at midlength. The sizes of the cutouts were changed to determine the effect on the buckling load. The current paper describes the details of the NASTRAN analysis, presents some of the analytical results, and makes a comparison with experimental results for the buckling of a typical isotropic cylinder with a circular cutout.

TEST CYLINDERS

Isotropic Cylinder

The isotropic cylindrical shell test specimen studied in this investigation was 25.4 cm long, had a shell radius of 10.2 cm and a wall thickness of 0.025 cm. The test specimen was made from Mylar[1] polyester film. The modulus of elasticity of this material was experimentally determined to be equal to 5.0 GN/m^2 and Poisson's ratio was taken from reference 5 to be equal to 0.3. A series of single circular cutouts with selected radii

[1]DuPont registered trademark.

ranging up to approximately 3.11 cm were cut into the cylinder wall at mid-length. Thick aluminum end plates were attached to the ends of the cylinder to provide a clamped end boundary condition. A concentrated compressive force was applied at the center of the top end plate.

Waffle Stiffened Cylinder

A large waffle stiffened cylindrical shell soon to be tested is illustrated in figure 1. The cylinder has a radius of 1.53 m, a length of 2.39 m, and a skin thickness of 0.25 cm. The cylinder material is aluminum which has a modulus of elasticity of 68.9 GN/m^2 and a Poisson's ratio of 0.333. The integral waffle stiffeners consist of circumferential rings and longitudinal stringers each with rectangular cross-section. A potential test configuration which was selected for the analytical study has two diametrically opposed rectangular cutouts of equal size located at the cylinder midlength. The rectangular cutouts have a circumferential arc length of 0.61 m and a longitudinal dimension of 0.69 m. The cylinder will be tested in axial compression in a test fixture which approximates clamped end boundary conditions.

NASTRAN MODELS

General Comments On Modeling and Boundary Conditions

A structural model should involve sufficient detail to represent accurately the physical problem yet be as simple as possible to reduce the computational cost. Since a curved plate element is not yet available in NASTRAN, a cylindrical shell must be modeled by the use of flat plate elements. This limitation requires that a relatively large number of circumferential grid points be used to obtain an accurate solution. In addition, it is the recommendation of reference 6 that NASTRAN quadrilateral plate elements be restricted to side dimension ratios between 1:1 and 1:1.5. Compliance with this recommendation requires that a correspondingly large number of gridpoints be used in the longitudinal direction.

The accuracy of the results for the buckling of cylinders without cutouts has been shown in reference 7 to depend on the number of grid points contained within a buckling mode half wave. These results indicate that approximately 3 grid points per half wave are required for an accuracy within 5 percent for stiffened cylinders,while approximately 5 grid points per half wave are required for an isotropic cylinder for the same accuracy. Reference 7 also suggests that the rotation about the radial axis be restrained at all grid points for cylinders modeled with flat plates. Low buckling loads are obtained if this restraint is not imposed because of the low inplane rotational stiffness of two nearly coplanar intersecting flat plates. This phenomenon is discussed further in reference 8.

The number of grid points necessary to model a structure accurately can be significantly reduced by taking advantage of existing loading and geometric symmetry. All of the models considered in this investigation had at least two planes of symmetry. For the model with one cutout at cylinder midlength, one plane of symmetry contained the cutout center and the cylinder axis of revolution,and the second plane passed through the cylinder at midlength normal to the axis of revolution. For cylinders containing two diametrically opposed holes at cylinder midlength, a third plane of symmetry exists which includes the axis of revolution and is normal to the cylinder diameter containing the two cutout centers. The applied loads were also symmetric since the concentrated load applied to the isotropic cylinder and the load resultant associated with the uniform end shortening of the waffle stiffened cylinder were collinear with the axis of revolution.

Taking advantage of these symmetry properties allows a cylinder with one cutout to be equivalently modeled by a one-quarter cylindrical segment and a cylinder with two cutouts to be represented by a one-eighth segment as illustrated in figure 2. These segments contain one true boundary (line 1 in figure 2) for which boundary conditions are prescribed to represent the actual edge conditions. In addition, there are three artificial boundary lines which have either symmetric or antisymmetric constraints imposed upon them. There are eight possible combinations of the symmetric and antisymmetric boundary constraints that can be imposed, and each combination should be considered to insure that the lowest eigenvalue has been found. In this

investigation results are presented only for symmetric boundary constraints.

The buckling capability provided by NASTRAN in Rigid Format 5 is a linear bifurcation buckling analysis for which the bifurcation occurs from a linear prebuckling state. This Rigid Format does not permit different prebuckling and buckling boundary conditions to be imposed. When the buckling of a thin cylindrical shell is approximated by a linear bifurcation buckling analysis, it is often necessary to impose different prebuckling and buckling boundary conditions. The buckling boundary conditions that are usually imposed for clamped or simple support conditions consist of one of the four sets of distinct boundary conditions at each end of the shell which accompany the formulation of the eighth order partial differential equation derived from classical shell theory. The capability of imposing different prebuckling and buckling boundary conditions was made possible in the present investigation through the use of a DMAP alter sequence which was provided by the NASTRAN Systems Management Office through the courtesy of Malcolm W. Ice of Boeing Computer Sciences, Inc. This DMAP sequence is presented in the appendix.

The prebuckling and buckling boundary conditions used in this investigation are presented in table I. The numbers 1, 2, and 3 in this table represent constrained displacements along the radial, circumferential and axial directions, respectively (see fig. 2) and the numbers 4, 5, and 6 represent constrained rotations about these three axes in a system of cylindrical coordinates. In this investigation one simple support and two clamped buckling boundary condition sets were examined. The prebuckling simple support boundary conditions allow uniform free expansion in the radial direction. The simple support buckling boundary condition set consisted of zero radial and circumferential displacements, zero edge bending moment, and a zero axial load perturbation. In the usual shell theory notation these conditions correspond to $w = v = M_x = N_x = 0$. The clamped prebuckling boundary conditions allowed axial displacements to occur freely and constrained all other edge displacements and slopes. One set of clamped buckling boundary conditions (case I) was identical to the prebuckling set. This is consistent in shell theory notation to setting $N_x = v = w = w_{,x} = 0$ where $w_{,x}$ represents the first derivative of the radial displacement with respect to the axial coordinate. The second clamped buckling boundary condition set

(case II) constrained all rotations and displacements. This is consistent in shell theory notation to setting $u = v = w = w_{,x} = 0$ where u represents the axial displacement.

Isotropic Cylindrical Models

Two NASTRAN modeling configurations were used to study the isotropic cylinder. The first configuration was a model of the complete cylinder without a cutout, and was used to determine the grid point network fineness necessary to provide an acceptable comparison with known analytical results. The uniformly spaced network of 720 grid points used for this model consisted of twelve axial stations and sixty circumferential stations. Following the suggestion of reference 7, the rotation about the radial axis was constrained for all grid points. The boundary conditions for this model were clamped case II as described above. The shell wall was modeled by CQUAD2 plate elements and the applied load resulted from imposing a uniform axial displacement.

The second model configuration was intended to simulate an experimental parametric study of the effect of a single unreinforced circular cutout on the buckling of a cylinder loaded by axial compression. Symmetry properties made it possible to represent this problem by an equivalent one-quarter cylindrical segment. A schematic representation of the cylinder geometry and end plate model is presented in figure 3(a). The aluminum end plate was modeled by a framework consisting of CBAR beam elements. The framework included one CBAR element between the grid point at the center of the end plate and each of the circumferential grid points on the shell boundary, and a CBAR element between each circumferential grid point around the cylinder boundary. The stiffness of these bar elements was extremely high (2.9 GN-m^2) to simulate the relative rigidity of the end plate. A concentrated axial force was applied at the grid point located at the center of the end plate.

The grid point network used for a typical circular cutout with radius a is presented in figure 3(b). An exploded view of the grid point refinement used in the vicinity of the cutout is presented in detail A. A very fine grid point network was used in the vicinity of the cutout to represent the high local prebuckling stress gradients shown to exist in this region by several authors (e.g., ref. 9 and 10). The extent of this highly refined

grid point network (detail A) was three hole radii and was guided by the prebuckling stress distribution presented in reference 9. Five cutout radii were considered ranging from approximately 0.406 cm to 1.27 cm and the corresponding models contained from 334 to 362 grid points. CQUAD2 and CTRIA2 plate elements were used to model the shell wall. Only symmetric boundary constraints were considered along the artificial boundary lines to limit the computational costs.

Waffle Stiffened Cylindrical Models

Four separate models were used in studying the buckling behavior of the waffle stiffened cylinder shown in figure 1. Details of the four models are presented in figure 4. The first configuration (model A) was a model of the complete cylinder without cutouts. The uniformly spaced network of 540 grid points used for this model consisted of nine axial stations and sixty circumferential stations. The second configuration (model B) was a one-eighth cylindrical segment with grid point spacing identical to model A and included 80 grid points. The third configuration (model C) was developed from model B by removing two grid points and the associated elements in order to represent two diametrically opposed cutouts at the cylinder midlength. The cutouts in the cylinder represented by model C were rectangular and have a circumferential arc length and axial length equal to 0.64 m and 0.60 m respectively. The actual cylinder shown in figure 1 was modeled using CQUAD2 flat plate elements to represent the skin and CBAR elements to represent the rings and stringers. Since the spacing of rings and stringers was closer for the actual cylinder than for model C, equivalent properties were assigned to the CBAR elements on the PBAR card. Each CQUAD2 element was bounded on all four sides by a CBAR element. The fourth configuration (model D) was also a one-eighth cylindrical segment representing a cylinder with two equal diametrically opposed rectangular cutouts. Two cutout sizes were considered for model D; one with dimensions 0.61 m by 0.69 m, and the other with dimensions 0.91 m by 0.69 m in the circumferential and axial directions, respectively. The grid point network in the vicinity of the hole was refined for model D such that a skin panel bounded by rings and stringers was represented by four CQUAD2 plate elements. CTRIA2 plate elements were used to make

the transition between regions of the shell with different grid point spacing. The grid point refinement in the vicinity of the hole was guided by the results for model C and by the high local prebuckling stress gradient expected to exist in this region. Model D contained 424 grid points. The hole edges for both models C and D were reinforced by rings and stringers with the properties identical to those used in the adjacent interior stiffener elements.

A uniform axial displacement was the applied loading condition for all four models. Boundary conditions used for these models included simple support, clamped case I, and clamped case II conditions as described in table I. The rotation about the radial axis was constrained for all grid points. Only symmetric boundary constraints were considered along the artificial boundary lines of models B, C, and D.

RESULTS

Isotropic Cylinders

The results of the NASTRAN study on the effects of a circular cutout on the buckling of a cylindrical shell loaded in axial compression are compared in figure 5 with some typical experimental results taken from reference 1. The buckling loads, P, of these studies have been nondimensionalized by the classical theoretical buckling load, P_{CL}, of a cylindrical shell without a cutout. These normalized buckling loads are plotted as a function of a nondimensional geometric parameter

$$r = a/(Rt)^{1/2}$$

where a is the cutout radius, R is the shell radius, and t is the shell thickness. Analytical prebuckling solutions (e.g., ref. 9) and experimentally determined buckling loads have been shown to be related to this parameter.

The experimental results indicate that it is possible to identify ranges of the parameter r for which there were different buckling characteristics. For r less than approximately 0.5, it appears that there was no effect of the cutout on the experimental buckling load, and the familiar general collapse diamond pattern was always the buckling mode

(represented by square symbols on figure 5). For values of r between approximately 0.5 and 1.2 there was a sharp decline in the buckling load, and the shell still buckled in the general collapse pattern. It is suggested in reference 1 that the prebuckling stress concentration around the hole is apparently of sufficient magnitude to cause the hole region to snap into a local buckling configuration which could in turn provide enough of a disturbance at these applied stress levels to cause general collapse. For values of r greater than approximately 1.2 a stable local buckling mode occurred in the vicinity of the hole (represented by circular symbols on figure 5) which was followed by the general collapse of the shell when a small additional load was applied. The buckling loads continue to decline in this range as r is increased but at a much lower rate than for the previous range. For the larger values of r, visible local prebuckling deformations normal to the shell surface were observed in the region of the cutout implying a local nonlinear prebuckling behavior.

The buckling load from NASTRAN for the complete cylindrical model without a cutout was fourteen percent greater than the classical theoretical value. The mode shape consisted of fourteen circumferential half waves and one axial half wave. The model therefore had approximately four grid points per circumferential half wave. The solution took 4079 CPU seconds with a core storage of 300000_8 words on a Control Data Corporation 6600 computer. A greater refinement in the circumferential direction did not appear worth the cost. One suggestion for reducing the CPU time required to obtain a solution might be to reduce the number of axial grid points since for the present solution there were twelve grid points per axial half wave. However, this would increase the ratio of side lengths of the quadrilateral elements to values well above those recommended in reference 6 and the accuracy of the resulting solution may be questionable.

The NASTRAN results for the equivalent one-quarter cylindrical segment model for cylinders with cutouts are represented by the dashed curve on figure 5. The buckling mode shape predicted by NASTRAN for all cases considered was a local buckling mode in the region of the cutout. The existence of this local buckling mode shape gives credence to the suggestion that general collapse in the experiment was caused by a local buckling mode for

values of r between 0.5 and 1.2. For values of r less than approximately 1.5 the NASTRAN results provided an upper bound for the experimental results as should be expected from a solution technique based on the minimization of the total potential energy. For larger values of r the nonlinearities of the cutout problem become more pronounced and the linear bifurcation analysis provided by NASTRAN gives results below the experimental values. The limitations of using a linear bifurcation analysis to approximate a nonlinear buckling phenomenon are pointed out in reference 4 in which a comparison is made between linear and nonlinear buckling solutions for some typical thin shell structures (e.g., the collapse of a cylindrical panel due to an applied concentrated lateral load).

Waffle Stiffened Cylinders

A summary of the NASTRAN results for models of the waffle stiffened cylinder illustrated in figure 1 is presented in table II, and includes eight different cases. The critical buckling loads calculated using NASTRAN are normalized by the buckling load for a stiffened simply supported cylinder without cutouts obtained from the analysis presented in reference 11. A bar graph is presented in figure 6 to illustrate graphically the differences in results for the eight different solutions.

The NASTRAN results for the complete cylinder without holes (model A) with simple support end conditions was within two percent of the reference buckling load. The one-eighth cylindrical segment (model B) with simple support end constraints also agreed with this result, indicating that the symmetric constraints applied along the artificial boundary lines yielded the minimum solution. A NASTRAN generated plot of the buckling mode shape for models A and B is presented in figure 7. The mode shape included one longitudinal and eight circumferential half waves, which was the same as predicted by reference 11. The CPU time to generate these two results was 5.5 minutes for model B and 79 minutes for model A. Although all eight combinations of symmetry and antisymmetry were not executed for model B, it is projected that even if they had been, the cumulative time would have been less than that required for the solution for the entire cylinder (model A). In addition, a larger core storage is required for the execution of the entire cylinder model.

Buckling results obtained using models C and D for a simply supported cylinder containing two diametrically opposed holes are presented in table II as cases 3 and 4. The hole sizes for these two models were slightly different due to differences in modeling. The critical compressive buckling loads are in relatively close agreement (within eight percent). Contour plots of the buckling mode shapes for the two models is presented in figure 8. Displacements have been normalized with respect to the maximum displacement amplitude which has been scaled to a value of 100. A discussion of the contour plotting technique is presented in reference 12. These two mode shapes are similar in character with the largest displacements occurring in the vicinity of the cutout. Although it is assumed for this solution that symmetric constraints exist along the three artificial boundaries (lines 2, 3, and 4 in figure 2), it may be assumed from a study of the displacement contour plots that it probably would not be necessary to exercise all eight combinations of symmetric and antisymmetric constraints to obtain the lowest eigenvalue. For example, an antisymmetric constraint along line 2 should yield essentially the same result as a symmetric constraint along this line since the magnitudes of the buckling displacements in the vicinity of line 2 are relatively small. The difference in the critical buckling load for models C and D with clamped case I boundary conditions (cases 5 and 6) was twelve percent. As for the simple support case, the buckling mode shapes were similar.

There was approximately a five percent decrease in the buckling load for cylinders with clamped case II boundary conditions (cases 7 and 8 in table II) when the circumferential hole dimension was increased by approximately fifty percent. Apparently, the rings and stringers in the vicinity of the hole are sufficiently stiff to allow a redistribution of the prebuckling stress to prevent significant decreases in the buckling load.

CONCLUDING REMARKS AND RECOMMENDATIONS

NASTRAN has been used to study the complex problem of the buckling of cylindrical shells with and without cutouts. Reasonably acceptable agreement with known analytical results was achieved for isotropic and waffle stiffened cylinders without cutouts when the appropriate prebuckling and buckling boundary conditions were imposed. The capability of imposing different prebuckling and buckling boundary conditions (which is usually required for a linear bifurcation buckling analysis) was made possible through the use of a DMAP alter sequence. For isotropic cylinders with cutouts it was found that NASTRAN provided an upper bound for available experimental results for small cutouts, and provided solutions lower than the experimental results for large cutouts. For the large cutouts, the nonlinearities of the problem become pronounced, and therefore the linear bifurcation buckling analysis capability of NASTRAN cannot be expected to provide more than an approximation to the solution.

The computational cost of conducting a buckling analysis for a structure is several times the cost of performing a static stress analysis for the same model. Therefore, the user of Rigid Format 5 should seriously consider ways to reduce computational costs and the potentially high demands placed on the computational facility. In general, taking advantage of problem loading and geometric symmetries can reduce the cost of preforming a buckling analysis. An argument can also be made that it is usually cost effective to select an eigenvalue search range on the EIGB card which is less than the expected eigenvalue to insure that the lowest root is obtained and therefore, that a restart is not required. It is recognized that some modules within the Rigid Format 5 DMAP sequence have greater storage requirements than others. Additional computational cost reductions and improvements in facility management could be made if it were possible to determine core storage requirements for certain DMAP modules before the module is executed. With this information it would be possible to adjust core storage requirements during the execution of a problem to a specified minimum and therefore release unnecessary core. This capability might be achieved automatically on certain computer systems or by the user through exercising the NASTRAN checkpoint and restart feature.

The systematic approach used in formulating a NASTRAN model simplifies the task of generating input data for general shells with complex geometries. Solutions for thin shell buckling problems by the use of NASTRAN, however, require an understanding of structural behavior to interpret properly the results. Therefore, NASTRAN must be used with discretion to obtain buckling loads for general shell structures because of the complexity of the problem, and the limited reported user experience for these problems.

APPENDIX

DMAP ALTER SEQUENCE FOR PRESCRIBING DIFFERENT PREBUCKLING AND BUCKLING BOUNDARY CONDITIONS

```
ALTER  2
FILE   KDGG=APPEND,SAVE/KNN=SAVE/GM=SAVE $
ALTER     47
LABEL     POINT1 $
ALTER     80
PARAM     //C,N,SUB/V,N,TEST1/C,N,2/V,N,NSKIP $
COND      POINT2,TEST1 $
*ALTER    104
PARAM     //C,N,MPY/V,N,NSKIP/C,N,2/C,N,1 $
REPT      POINT1,1 $
LABEL     POINT2 $
ENDALTER
```

* - Use ALTER 109 for level 15 or 104 for level 12.

The execution of the alter sequence requires three subcases in the Case Control Deck. Subcase 1 governs the prebuckling solution and subcases 2 and 3 govern the buckling solution.

```
SUBCASE 1
LOAD =
SPC =
MPC =
OUTPUT

SUBCASE 2
METHOD =
OUTPUT

SUBCASE 3
SPC =
MPC =
OUTPUT
```

REFERENCES

1. Starnes, J. H.: The Effect of a Circular Hole on the Buckling of Cylindrical Shells. Ph. D. Thesis, California Institute of Technology, 1970.

2. Tennyson, R. C.: The Effects of Unreinforced Circular Cylindrical Shells Under Axial Compression. Journal of Engineering for Industry. November 1968, pp. 541-546.

3. Brogan, F.; and Almroth, B.: Buckling of Cylinders with Cutouts. AIAA Journal, Vol. 8, No. 2, February 1970, pp. 236-240.

4. Almroth, B. O.; and Brogan, F. A.: Bifurcation Buckling as an Approximation of the Collapse Load for General Shells. AIAA Journal, Volume 10, No. 4, April 1972, pp. 463-467.

5. Seide, P.; Weingarten, V. I.; and Morgan, E. J.: The Development of Design Criteria For Elastic Stability of Thin Shell Structures. AFBMD/TR-61-7, U. S. Air Force, December 31, 1960.

6. Haggenmacher, Gernot W.: Some Aspects of NASTRAN Solution Accuracy. NASTRAN: Users' Experiences. NASA TM X-2378, 1971, pp. 47-63.

7. Brolliar, Richard H.: A NASTRAN Buckling Analysis of a Large Stiffened Cylindrical Shell with a Cutout. NASTRAN: Users' Experiences. NASA TM X-2378, 1971, pp. 65-84.

8. Zienkiewicz, O. C.: The Finite Element Method in Engineering Science. McGraw-Hill Book Company Inc., 1971, pp. 212-238.

9. Lekkerkerker, J. G.: On the Stress Distribution in Cylindrical Shells Weakened By a Circular Hole. Ph. D. Thesis, Technological University, Delft, Netherlands, 1965.

10. Savin, G. N.: Stress Distribution Around Holes. NASA TT F-607, 1970.

11. Block, David L.; Card, Michael F.; and Mikulas, Martin M., Jr.: Buckling of Eccentrically Stiffened Orthotropic Cylinders. NASA TN D-2960, 1965.

12. Giles, Gary L.; and Blackburn, Charles L.: Procedure for Efficiently Generating, Checking, and Displaying NASTRAN Input and Output Data for Analysis of Aerospace Vehicle Structures. NASTRAN: Users' Experiences. NASA TM X-2378,1971, pp. 679-696.

TABLE 1.- BOUNDARY CONDITIONS.

	Constrained displacements and rotations[a]	
	Prebuckling	Buckling
Simple support - line 1[b]	2,4,6	1,2,4,6
Clamped case I - line 1	1,2,4,5,6	1,2,4,5,6
Clamped Case II - line 1	1,2,4,5,6	1,2,3,4,5,6
Symmetry - line 2 or 4	2,4,6	2,4,6
Symmetry - line 3	3,4,5	3,4,5
Antisymmetry - line 2 or 4	2,4,6	1,2,4
Antisymmetry - line 3	3,4,5	1,3,4

a.- Numbers 1,2, and 3 represent radial, tangential, and axial displacements and 4,5, and 6 represent rotations about these axes, respectively in a cylindrical coordinate system.

b.- Lines 1,2,3, and 4 are defined in figure 1.

TABLE II.- NASTRAN BUCKLING RESULTS FOR A WAFFLE STIFFENED CYLINDRICAL SHELL.

CASE	MODEL	HOLE DESCRIPTION[a]	LOADING	END BOUNDARY CONDITION[b]	$\frac{P^c}{P_{ref}}$
1	A	no hole	uniform displacement, top and bottom	simple support	1.02
2	B	no hole	uniform displacement of top (line 1)	simple support	1.02
3	C	2 holes, 0.64 m x 0.60 m	uniform displacement of top (line 1)	simple support	0.712
4	D	2 holes, 0.61 m x 0.69 m	uniform displacement of top (line 1)	simple support	0.774
5	C	same as case 3	uniform displacement of top (line 1)	clamped case I	0.767
6	D	same as case 5	uniform displacement of top (line 1)	clamped case I	0.875
7	D	same as case 5	uniform displacement of top (line 1)	clamped case II	0.957
8	D	2 holes, 0.91 m x 0.69 m	uniform displacement of top (line 1)	clamped case II	0.905

[a] Hole size for complete cylinder located at midlength, two holes π radians apart, circumferential by axial dimensions.

[b] Where applicable, symmetric constraints were imposed along all three artificial boundary lines.

[c] The reference load is for a simply supported orthotropic cylinder without holes (reference 11). P_{ref} = 7.48 MN.

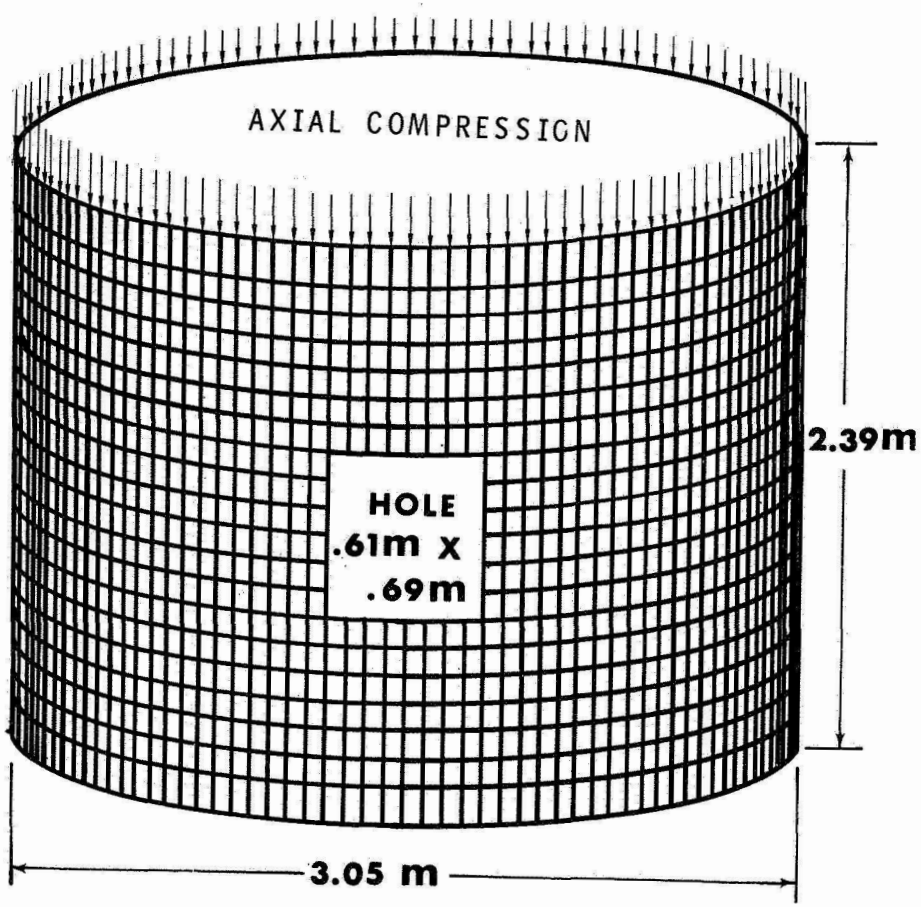

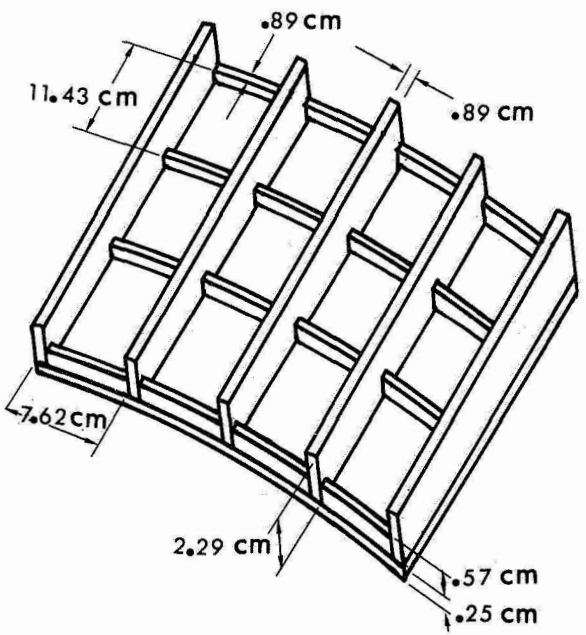

WAFFLE DETAIL

Figure 1.- Waffle stiffened cylinder containing two diametrically opposed holes located at midlength and π radians apart.

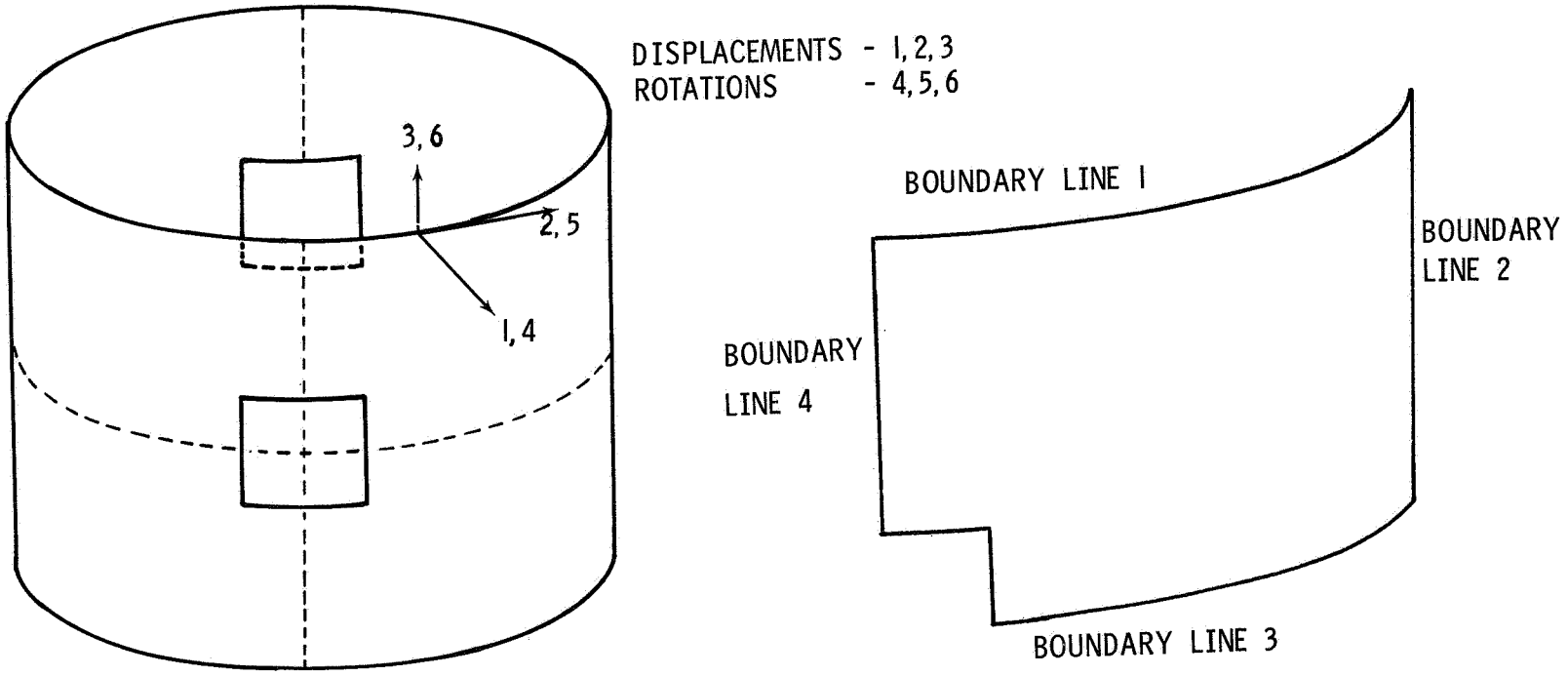

Figure 2.- Illustration of symmetry segmenting technique.

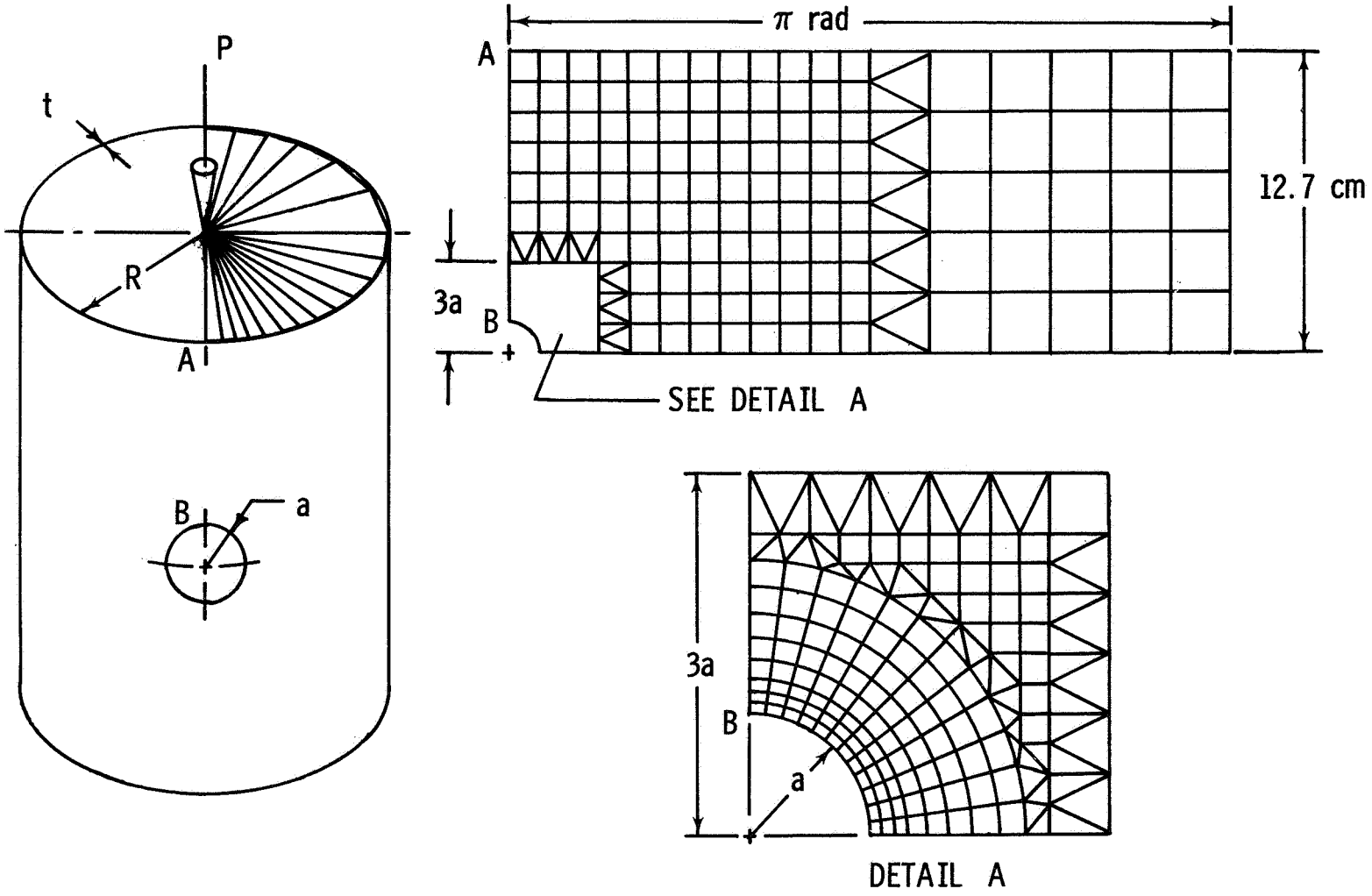

(a) Model Schematic

(b) Grid Point Network

Figure 3.- Model of isotropic cylinder with a circular cutout.

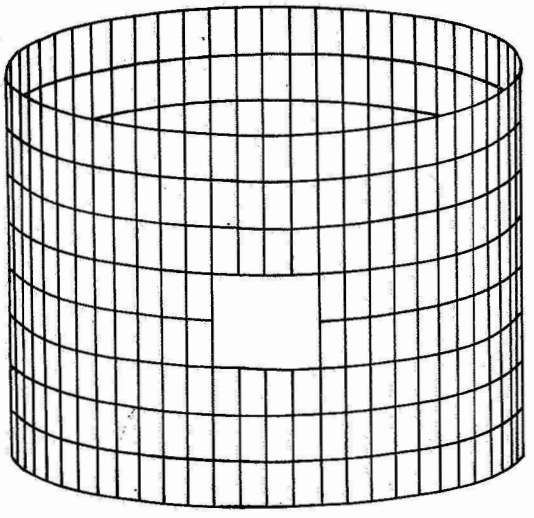

Model A

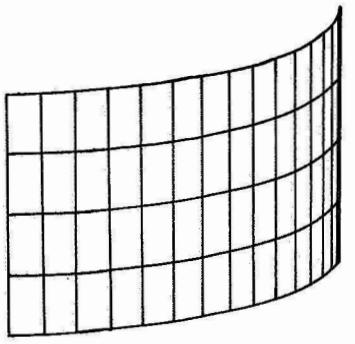

Model B

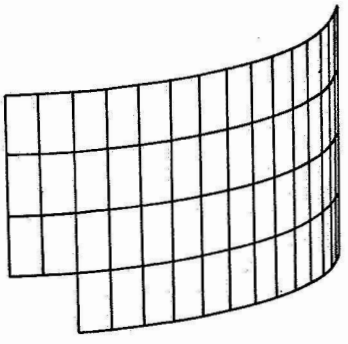

Model C

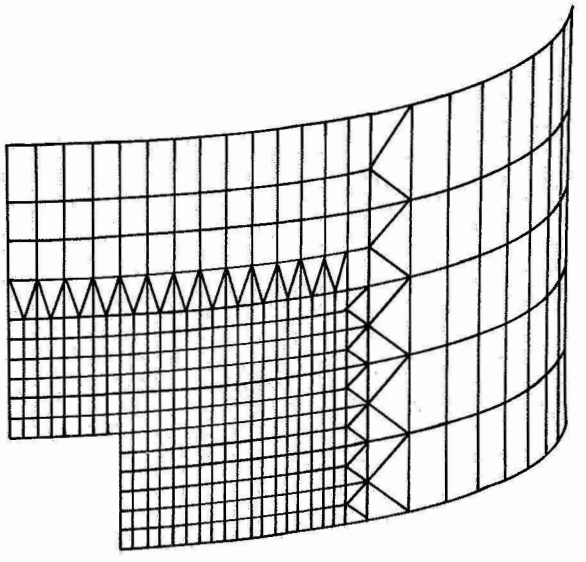

Model D

Figure 4.- Waffle stiffened cylindrical shell NASTRAN models.

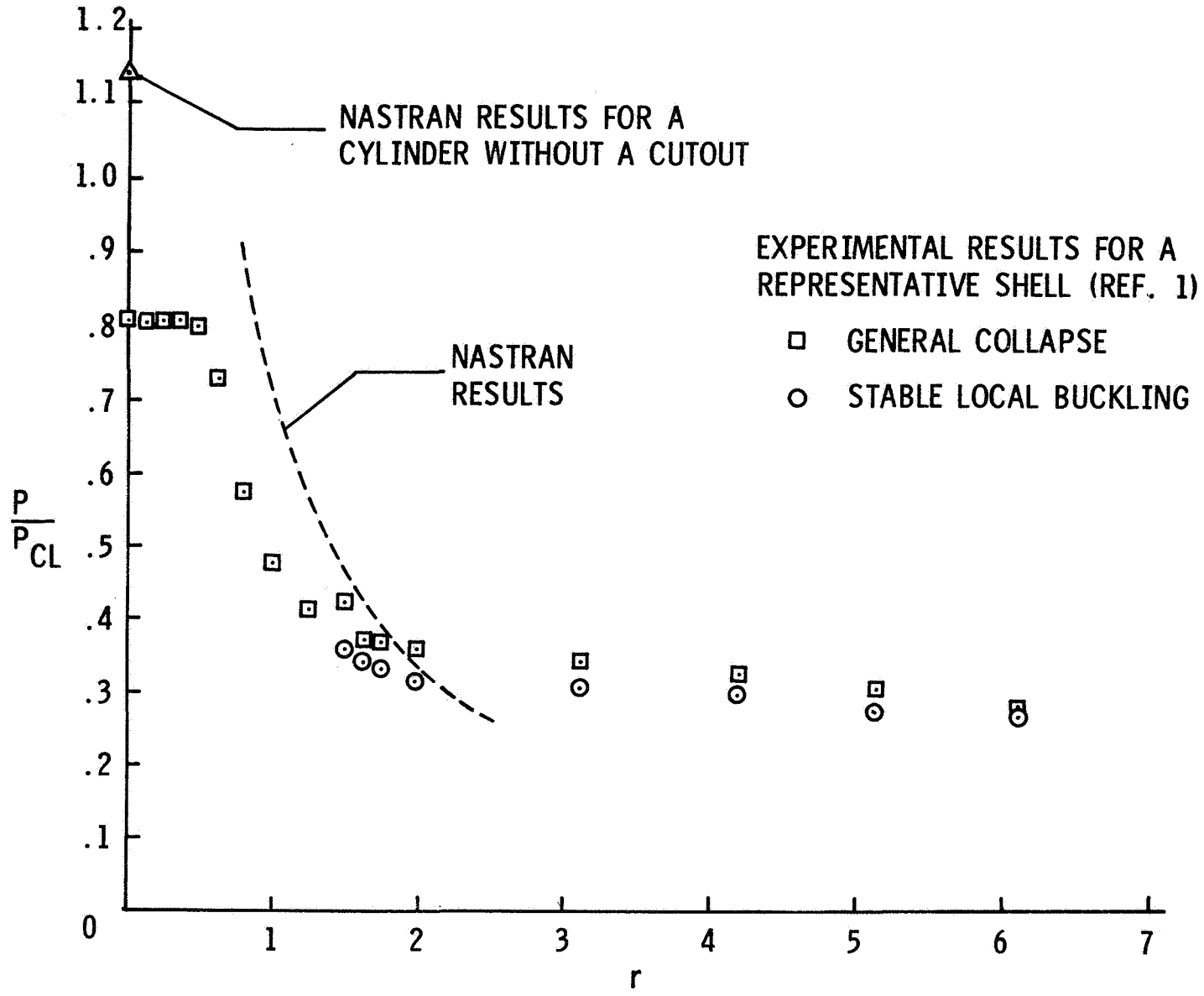

Figure 5.- Effect of circular cutout size on isotropic cylindrical shell buckling load where r is equal to $a/(Rt)^{1/2}$.

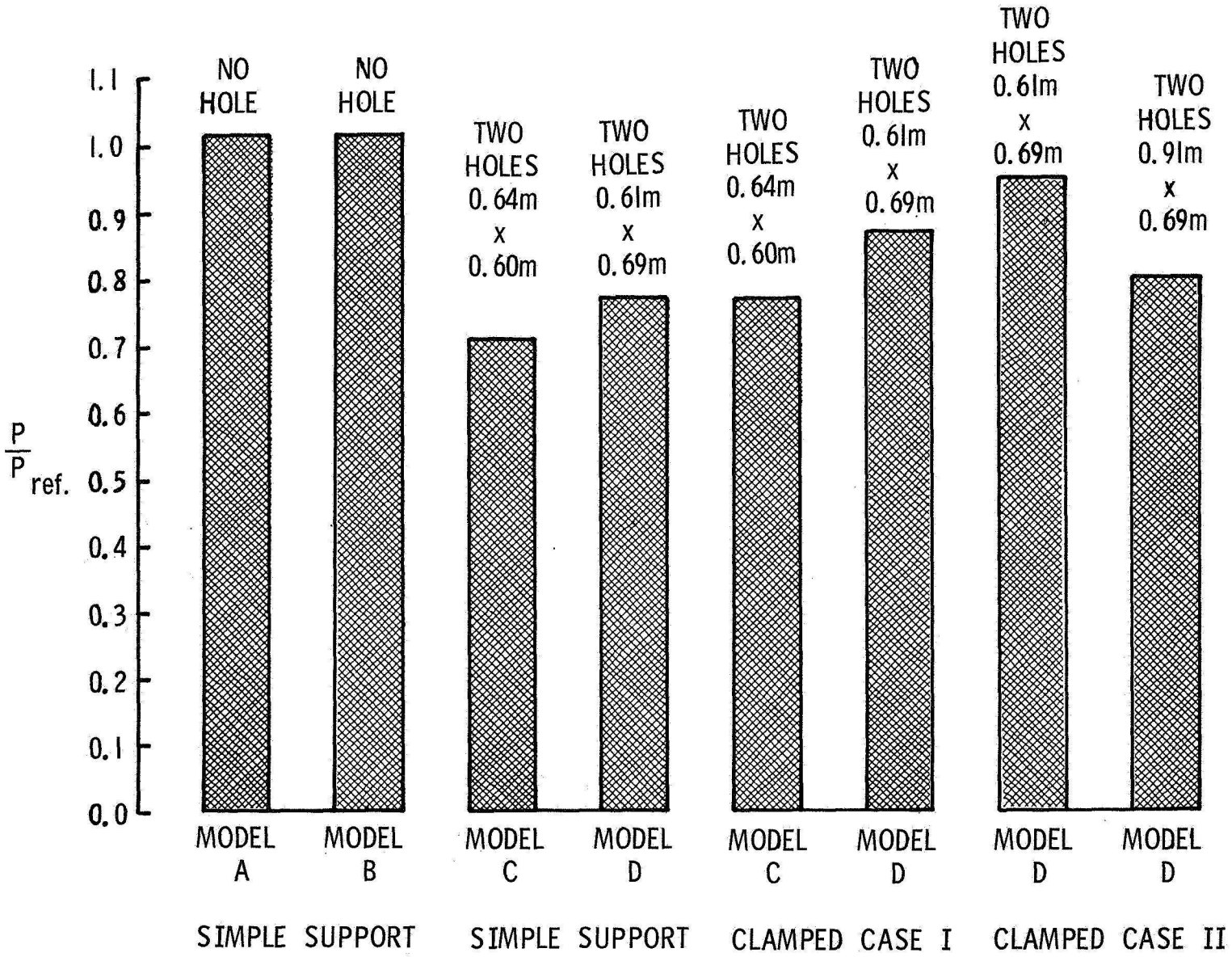

Figure 6.- Critical buckling load for waffle stiffened cylinders subjected to uniform axial displacement loading.

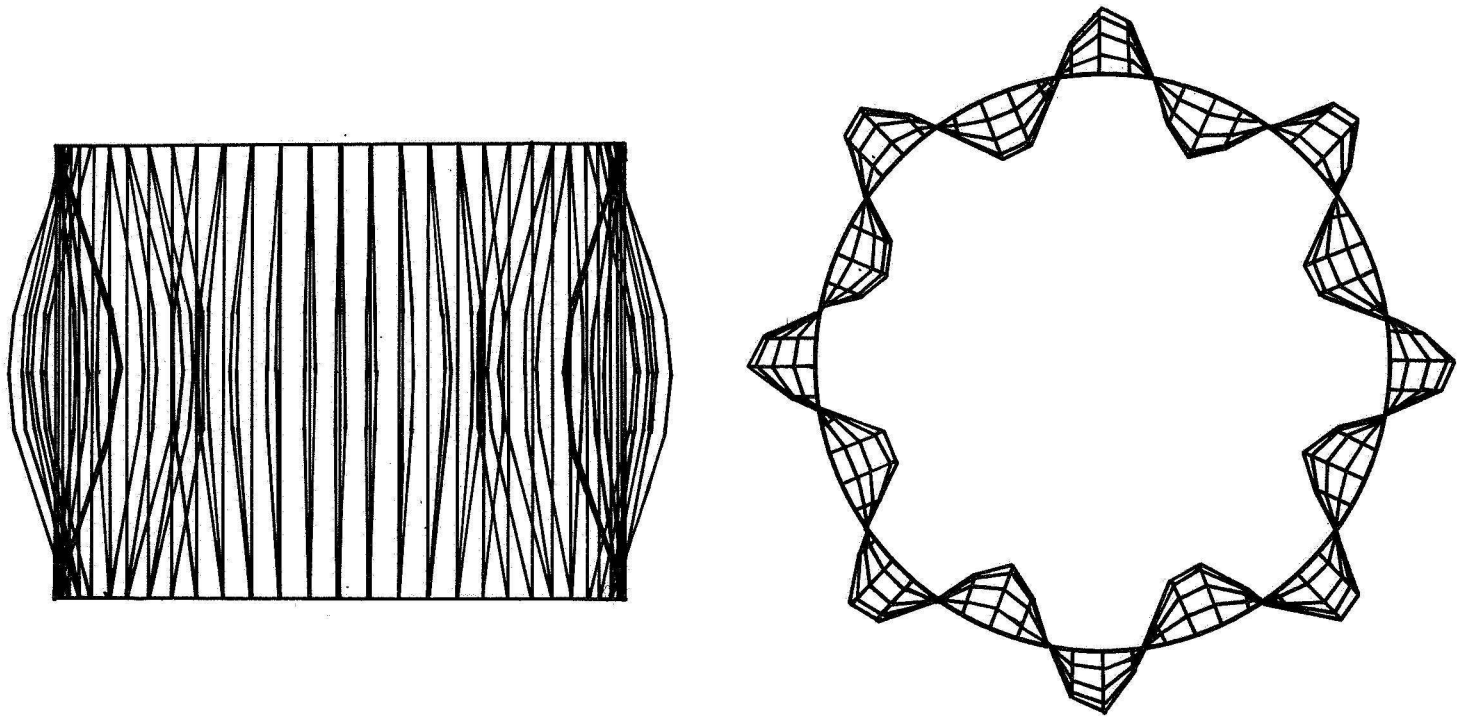

(a) Model A Results.

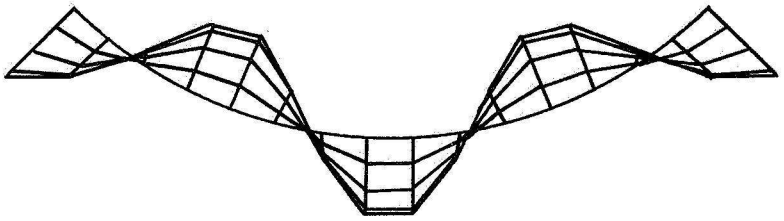

(b) Model B Results.

Figure 7.– Buckling mode shapes for waffle stiffened cylindrical shell showing identical results for models A and B.

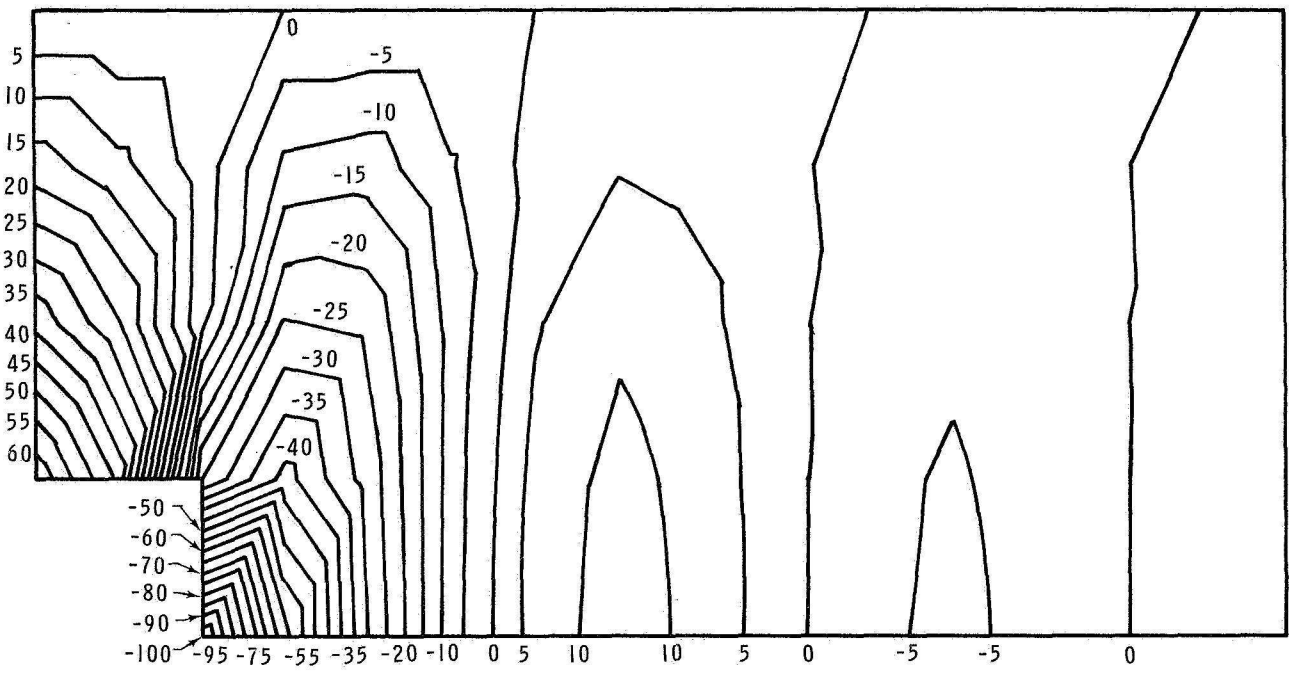

(a) Model B.

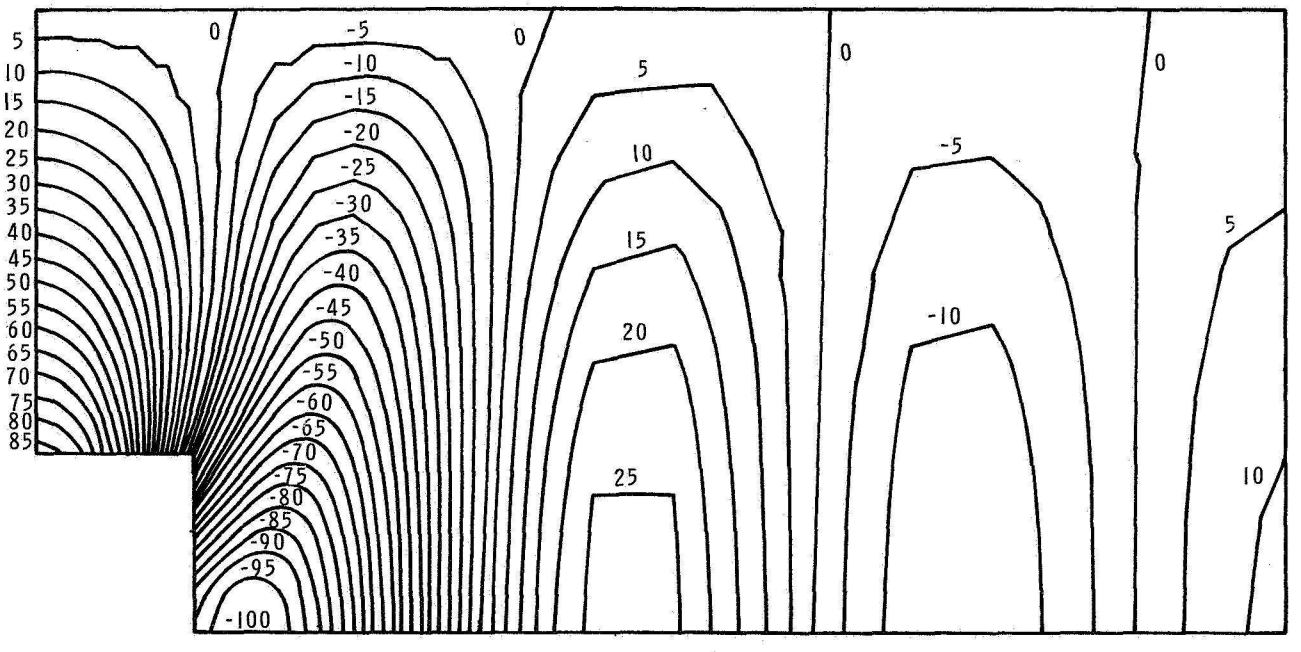

(b) Model C.

Figure 8.- Radial buckling displacement contour plot for a one-eighth segment of a simply supported waffle stiffened cylinder. All displacements scaled to a maximum displacement of 100.